iScience

CellPress
OPEN ACCESS

Article

Ctnnb1/β-catenin inactivation in UCP1-positive adipocytes augments the browning of white adipose tissue

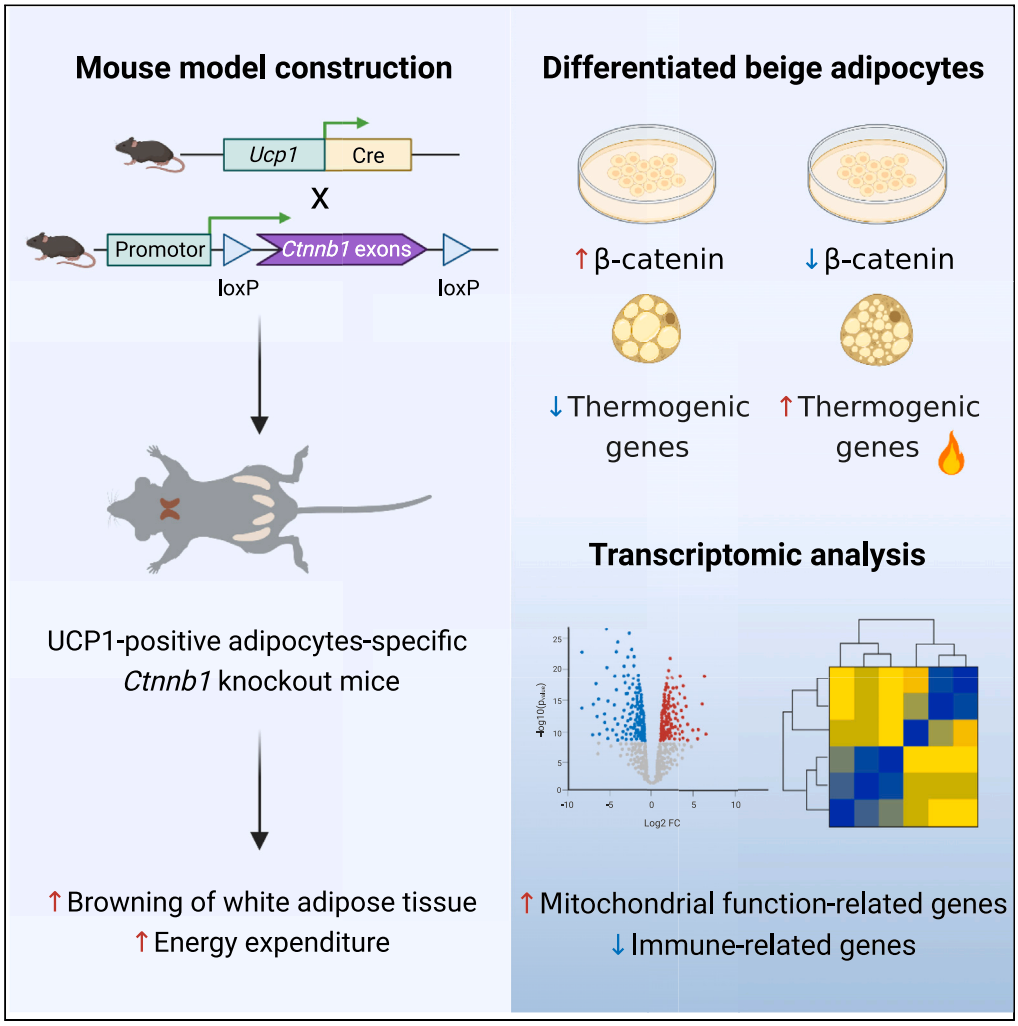

Na Chen, Mingyang Yuan, NingNing Zhang, Maopei Chen, Ruixin Liu, Jiqiu Wang, Peng Lu

sibslp@126.com (P.L.)
wangjq@shsmu.edu.cn (J.W.)
xiner198287@163.com (R.L.)

Highlights

Ctnnb1 deficiency in UCP1-positive adipocytes promotes browning of WAT

β-catenin inhibits thermogenic genes expression in beige adipocytes

50-week-old UBKO mice have improved metabolic performance

Chen et al., iScience 26, 106552
May 19, 2023
https://doi.org/10.1016/j.isci.2023.106552

iScience

CellPress
OPEN ACCESS

Article

Ctnnb1/β-catenin inactivation in UCP1-positive adipocytes augments the browning of white adipose tissue

Na Chen,[1,2,5] Mingyang Yuan,[1,2,5] NingNing Zhang,[1,2] Maopei Chen,[3] Ruixin Liu,[1,2,*] Jiqiu Wang,[1,2,*] and Peng Lu[4,6,*]

SUMMARY

Canonical WNT pathway in mature adipocytes exacerbates obesity. In this study, we constructed UCP1-positive adipocytes-specific *Ctnnb1* knockout mice (UBKO) and observed increased "browning" of white adipose tissue (WAT) following cold exposure or CL-316,243 administration compared to controls. UBKO mice also displayed increased energy expenditure. Furthermore, β-catenin (encoded by *Ctnnb1*) inhibited thermogenic genes expression in differentiated beige adipocytes and repressed *Ucp1* expression at transcription level. Transcriptome analysis revealed UBKO mice treated with CL-316,243 had enhanced mitochondrial function and downregulated immune-related genes in epididymal WAT. Improved glucose tolerance and insulin sensitivity were observed in 50-week-old UBKO mice. Public datasets indicated that *CTNNB1* expression was inversely correlated with several thermogenic genes expression in human adipose tissue/adipocytes and positively correlated with BMI or waist-hip ratio (WHR). We proposed that intervention of β-catenin in adipocytes could be an effective strategy to enhance energy expenditure and improve age-related metabolic performance.

INTRODUCTION

Obesity is a chronic public health problem that is often accompanied by abnormal glucose and lipid metabolism, increasing the risk of metabolic diseases including diabetes, fatty liver, cardiovascular disease, and a variety of cancers. The exacerbation of the epidemic trend of obesity has brought a serious burden to human health and the social economy.[1,2] Current intervention strategies for obesity include bariatric surgery and drugs; however, the effectiveness of most drugs is limited and they often come with adverse reactions.[3] Therefore, there is a need to find new therapies that can either reduce energy intake or increase energy consumption for the treatment of obesity.

Brown adipose tissue (BAT) has been identified in adult humans, and browning of white adipose tissue (WAT) is considered a promising strategy for obesity treatment.[4–6] A recent clinical trial confirmed that mirabegron, a β3-adrenergic receptor (β3-AR) agonist approved for treating overactive bladder, can increase brown fat in humans.[7] Chronic cold exposure or β3-AR agonist CL-316,243 can induce beige adipocytes formation in WAT, which has similar morphological features to classical BAT.[8] These findings support further investigation of the regulatory events involved in beige adipocytes formation and identity maintenance. Several studies have demonstrated that brown adipocytes and beige adipocytes originate from different precursor cells,[9–11] and their thermogenic mechanisms differ to some extent.[12,13] As beige adipocytes are a reversible cell type, the mechanisms of cell recruitment and identity maintenance remain largely unclear.

Adipogenesis is a highly sequential and dynamic process that is regulated by multiple transcription factors and co-factors. Canonical WNT/β-catenin pathway activation in the early stage of cell differentiation can block both white and brown adipogenesis.[14] β-catenin, encoded by *Ctnnb1*, functions as a key intracellular signal transducer in the WNT signaling pathway. To regulate target genes expression, β-catenin interacts with transcription factors such as transcription factor 7-like 2 (TCF7L2), hypoxia-inducible factor 1α (HIF1α), and forkhead box protein O (FOXO).[15] Changes in its activity have been linked to obesity and other metabolic diseases.[16,17] Recently, we found that *Ctnnb1* deficiency in mature adipocytes could resist high-fat

[1]Department of Endocrine and Metabolic Diseases, Shanghai Institute of Endocrine and Metabolic Diseases, Ruijin Hospital, Shanghai Jiao Tong University School of Medicine, Shanghai 200025, China

[2]Shanghai National Clinical Research Center for Metabolic Diseases, Key Laboratory for Endocrine and Metabolic Diseases of the National Health Commission of the PR China, Shanghai National Center for Translational Medicine, Shanghai 200025, China

[3]Liver Cancer Institute, Zhongshan Hospital, Fudan University and Key Laboratory of Carcinogenesis and Cancer Invasion, Ministry of Education, Shanghai 200032, China

[4]Department of Endocrinology, Shandong Provincial Hospital Affiliated to Shandong First Medical University, Shandong 250021, China

[5]These authors contributed equally

[6]Lead contact

*Correspondence: sibslp@126.com (P.L.), wangjq@shsmu.edu.cn (J.W.), xiner198287@163.com (R.L.)

https://doi.org/10.1016/j.isci.2023.106552

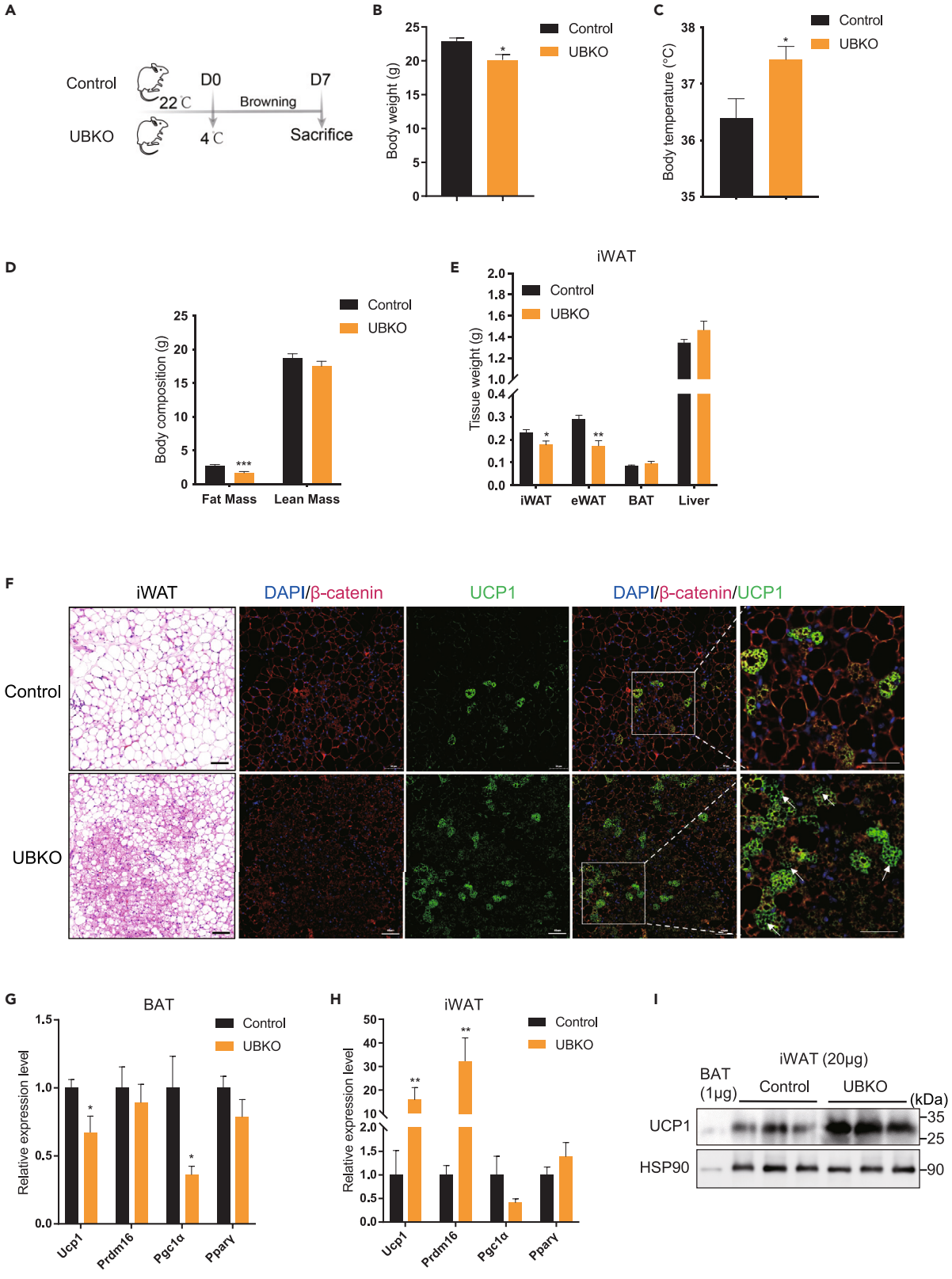
A
Control
UBKO
22 C
D0
Browning
D7
4 C
Sacrifice
B
Body weight (g)
Control
UBKO
C
Body temperature (°C)
Control
UBKO
D
Body composition (g)
Control
UBKO
Fat Mass
Lean Mass
E
iWAT
Tissue weight (g)
Control
UBKO
iWAT
eWAT
BAT
Liver
F
iWAT
DAPI/β-catenin
UCP1
DAPI/β-catenin/UCP1
Control
UBKO
G
BAT
Relative expression level
Control
UBKO
Ucp1
Prdm16
Pgc1α
Pparγ
H
iWAT
Relative expression level
Control
UBKO
Ucp1
Prdm16
Pgc1α
Pparγ
I
iWAT (20μg)
BAT (1μg)
Control
UBKO
(kDa)
UCP1
HSP90
35
25
90

Figure 1. Ablation of *Ctnnb1* in UCP1-positive adipocytes promotes the inguinal WAT "browning" under cold exposure

(A) The schematic diagram for 7-day chronic coldness exposure.

(B–E) Body weight (B), body temperature (C), body composition (D), and tissue weight (E) of UBKO and control male mice (n = 8 for each group).

(F) H&E staining and immunolabeling for β-catenin and UCP1 of sections of iWAT depots from control and UBKO mice. Scale bars, 50 μm (n = 3 for each group).

(G and H) mRNA levels of thermogenic genes in BAT (G) and iWAT (H) of UBKO and control male mice. (n = 8 for each group).

(I) Expression of UCP1 protein in the iWAT of UBKO and control male mice (20 μg of total protein from tissue lysate was loaded onto gel). WT BAT lysate (1 μg) was loaded as a control. (n = 3 for each group). For B–I, 8-week-old UBKO and control male mice were placed under 4°C for 7 days. Data are shown as means ± SEM. *p < 0.05, **p < 0.01, ***p < 0.001. See also Figures S1 and S2.

diet-induced obesity without affecting adipocyte identity, which was consistent with recent findings from the MacDougald group.[18,19] Canonical WNT pathway agonists could inhibit the expression of *Ucp1* in mature brown adipocytes without affecting other differentiation-related genes, such as *Pparγ*, *C/ebpα*, and *Fabp4*,[20] while it is noteworthy that *Adiponectin*-cre-driven *Ctnnb1* knockout in BAT has no impact on the expression of *Ucp1*,[19] which is the key effector of adaptive thermogenesis. These discrepancies across different models complicate the elucidation of the effects of the canonical WNT pathway on adipose tissue thermogenesis.

Our group previously reported that LGR4, an amplifier of WNT signaling, inhibited beige adipogenesis independent of the canonical WNT pathway.[21] In addition, genetic variations in *LRP5*, *RSPO3*, and *ZNRF3* have been implicated in association with waist-hip ratio (WHR).[16,22–24] The serial evidence indicates that components of the canonical WNT pathway play similar roles in adipogenesis but differ in their functions during various stages of adipocyte differentiation. However, the potential role of *Ctnnb1* in the process of WAT browning has not been explored. To further investigate the specific role of *Ctnnb1*/β-catenin in mature brown/beige adipocytes *in vivo*, a mouse model targeting β-catenin specifically is required.

Considering the heterogeneity of mature adipocytes, as revealed by recent single-nucleus RNA-sequencing studies,[25] here, we proposed using *Ucp1*-Cre-mediated *Ctnnb1* knockout (designated as UBKO mice) as a more suitable mouse model for investigating the role of β-catenin in thermogenic adipocytes in response to chronic cold exposure or CL-316,243 administration. Our data revealed that *Ctnnb1* depletion significantly promoted the browning of WAT both *in vivo* and *in vitro*. We performed bulk RNA sequencing to provide a comprehensive analysis of adipose tissue beyond the changes in thermogenic genes. In addition, UBKO mice had better glucose metabolism performance at 50 weeks old. Furthermore, we found an inverse correlation between *CTNNB1* expression and thermogenic genes in human adipocytes through analysis of public datasets. Collectively, our study provides valuable insights into the role of the canonical WNT pathway in energy expenditure.

RESULTS

Ablation of *Ctnnb1* in UCP1-positive adipocytes promotes the inguinal WAT "browning" under cold exposure

To investigate the role of β-catenin in brown/beige adipocytes, we generated a *Ucp1*-cre-driven *Ctnnb1* knockout mouse model (*Ucp1*-cre; *Ctnnb1*$^{flox/flox}$, UBKO) (Figure S1A) and confirmed an effective reduction of β-catenin in interscapular BAT (Figures S1B–S1D). Previous studies have suggested that the browning of WAT can occur spontaneously as early as peri-weaning and persist for approximately two weeks.[26] We performed H&E staining and immunofluorescence staining of UCP1 and β-catenin on inguinal WAT (iWAT) and epididymal WAT (eWAT) from postnatal day 25 (P25) control and UBKO mice. Beige adipocytes were present in both iWAT and eWAT (Figures S1E–S1H). More importantly, *Ctnnb1* knockout in UCP1-positive cells of UBKO mice occurred during this period (Figures S1F and S1H).

We subjected control and UBKO mice to a 7-day chronic cold exposure to evaluate the thermogenic capacity of WAT browning (Figure 1A). Following cold exposure, we observed a lower body weight and significant improvement in body temperature in UBKO mice compared to controls (Figures 1B and 1C). UBKO mice also showed a reduction in fat content, particularly in iWAT and eWAT, while no significant differences were observed in BAT and liver weight even after normalization to body weight (Figures 1D, 1E, S2A and S2B). H&E staining revealed that the iWAT of UBKO mice had more beige-like adipocytes with multilocular lipid droplets (Figure 1F). Immunofluorescence staining further confirmed that UBKO mice had more UCP1-positive adipocytes in iWAT, and β-catenin was knocked out in most UCP1-positive adipocytes (Figure 1F).

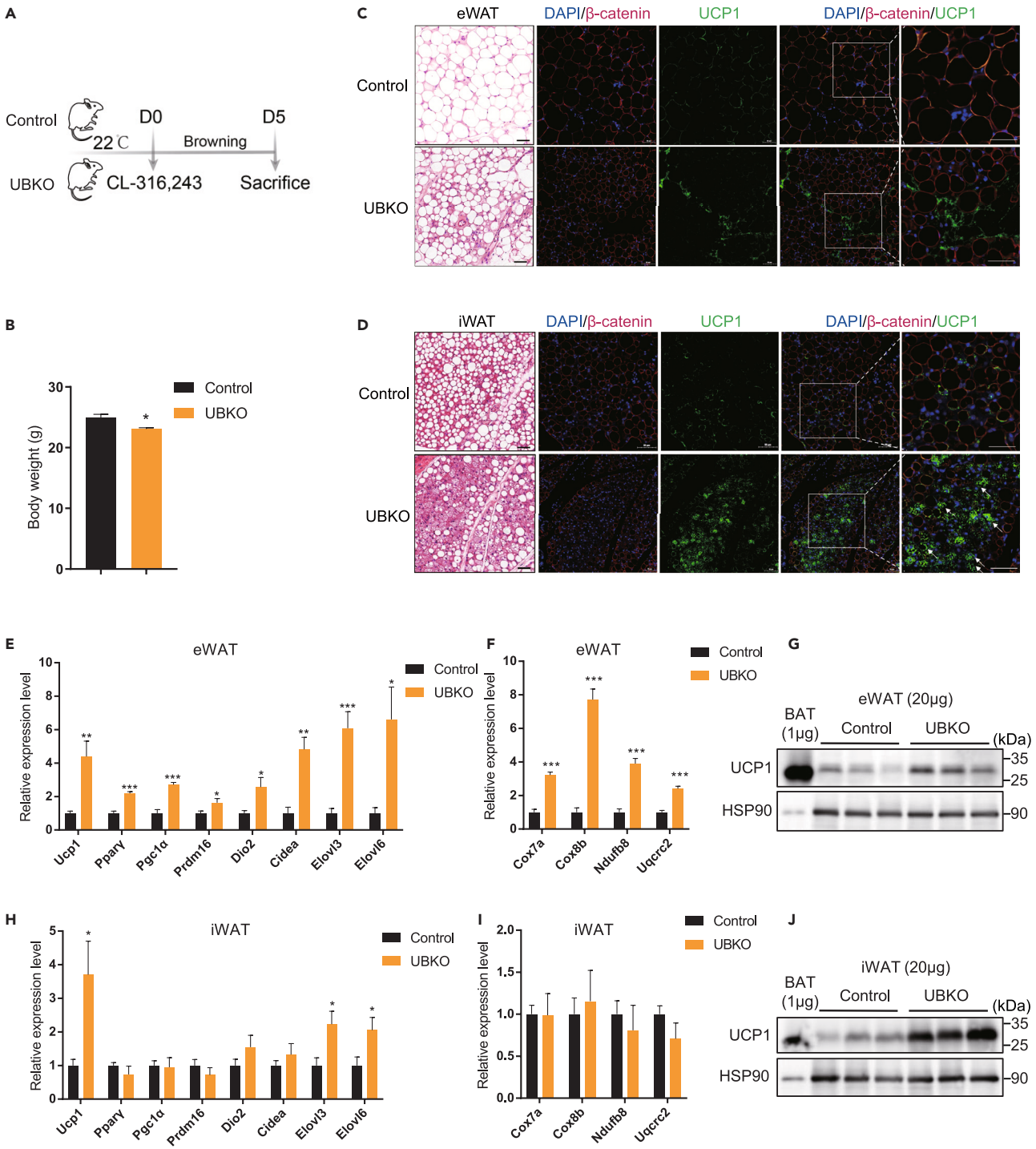

Figure 2. UBKO mice exhibit enhanced "browning" of WAT under the β3-adrenergic receptor agonist CL-316,243 administration

(A) The schematic diagram for the 5-day CL-316,243 treatment.

(B) Body weight of UBKO and control male mice (n = 4–5 for each group).

(C and D) H&E staining and immunolabeling for β-catenin and UCP1 of sections of eWAT (C) and iWAT (D) depots from control and UBKO mice. Scale bars, 50 μm (n = 3 for each group).

(E and F) mRNA levels of thermogenic (E) and mitochondrial function-associated (F) genes in the eWAT of UBKO and control male mice. (n = 4–5 for each group).

Figure 2. *Continued*

(H and I) mRNA level of thermogenic (H) and mitochondrial function-associated (I) genes in the iWAT of UBKO and control male mice. (n = 4–5 for each group).

(G and J) Expression of UCP1 protein in the eWAT (G) and iWAT (J) of UBKO and control male mice (20 μg of total protein from tissue lysate was loaded onto gel). WT 0.1 μg BAT lysate and 1 μg BAT lysate were loaded as control of eWAT and iWAT, respectively. (n = 3 for each group). For B–J, 8-week-old UBKO and control male mice were injected with CL-316,243 for 5 days. Data are shown as means ± SEM. *p < 0.05, **p < 0.01, ***p < 0.001. See also Figure S3.

We also analyzed the expression of thermogenic genes in iWAT and BAT. Interestingly, *Ctnnb1* deficiency did not improve the thermogenic program in BAT (Figure 1G). However, there was a significant increase in the expression of *Ucp1* and *Prdm16* genes and UCP1 protein in iWAT of UBKO mice (Figures 1H and 1I). In addition, we observed changes in some lipid metabolism-related genes in the iWAT of UBKO mice, but not in the BAT (Figures S2C and S2D). These results suggested that ablation of *Ctnnb1* in UCP1-positive adipocytes promotes the iWAT "browning" under cold exposure.

UBKO mice exhibit enhanced "browning" of WAT under the β3-adrenergic receptor agonist CL-316,243 administration

Previous studies reported that beige adipocytes may originate from *de novo* adipogenesis and white-to-brown *trans*-differentiation.[27,28] Cold exposure and CL-316,243 treatment, an agonist of the β3-adrenergic receptor, induce "browning" of WAT through different mechanisms.[29] In this study, we treated control and UBKO mice with CL-316,243 intraperitoneally for consecutive 5 days and then analyzed thermogenic genes expression in various adipose tissues (Figure 2A). Consistent with the effects of cold exposure, UBKO mice exhibited lower body weight (Figure 2B) after treatment with CL-316,243. Histological analysis revealed that β-catenin was knocked out in most UCP1-positive adipocytes, and UBKO mice had more UCP1-positive adipocytes in eWAT (Figure 2C) and iWAT (Figure 2D). In addition, UBKO mice had increased expression of thermogenic genes (Figures 2E, 2F, 2H, and 2I) and UCP1 protein (Figures 2G and 2J) in WATs, while there was no difference in BAT compared to control mice (Figures S3A and S3B). These results suggested that UBKO mice acquired a stronger capacity for WAT "browning" under the β3-adrenergic receptor agonist CL-316,243 treatment.

To evaluate the impact of *Ctnnb1* deficiency in UCP1-positive adipocytes on systemic energy metabolism, we measured oxygen consumption (VO_2), carbon dioxide production (VCO_2), energy expenditure, respiratory exchange ratio (RER), and physical activity in metabolic cages at the baseline condition without any stimulation. Our results showed that UBKO mice exhibited higher levels of O_2 consumption (Figures 3A and 3B), increased CO_2 production (Figures 3C and 3D), and greater energy expenditure (Figures 3E and 3F) compared to controls. Besides, there was no significant difference in RER (Figure S4A) or physical activity (Figure S4B) between the two groups. The improvement of energy expenditure in UBKO mice existed even adjusted for lean mass using ANCOVA analysis (Figure 3G).

β-catenin inhibits the expression of thermogenic and mitochondria-related genes *in vitro*

To further validate the effects of β-catenin on beige adipocytes, we constructed Flag-tagged constitutively active β-catenin (S33Y/S37F/T41A) adenovirus as previously reported[30,31] and infected differentiated beige adipocytes derived from iWAT stromal vascular fractions (SVFs) at day 2 after the core transcriptional program of adipogenesis was initiated. We detected the successful overexpression of β-catenin (Figures 4A and 4B) and increased expression of downstream genes *Axin2* and *Nkd1* (Figure S5A). Overexpression of β-catenin decreased the mRNA and protein expression of *Ucp1* and *Pgc1α*, as well as other thermogenic and mitochondria-related genes (Figures 4A and 4B). Furthermore, *Ctnnb1* knockdown promoted thermogenic and mitochondria-related genes expression *in vitro*, consistent with the findings in UBKO mice (Figures 4C and 4D). However, shRNA-mediated *Ctnnb1* knockdown in differentiated brown adipocytes derived from wild-type C57BL/6 mice showed no effect on *Ucp1* but increased *Pgc1α* expression (Figure S5B). As β-catenin is the core transcriptional co-factor in the canonical WNT pathway, we speculated that β-catenin inhibited *Ucp1* expression at transcriptional level. We overexpressed mouse *Ucp1*-promoter-driven luciferase in 293T cells and found that β-catenin significantly suppressed the transcriptional activity of m*Ucp1* promoter while IWR-1-endo, a WNT pathway inhibitor that promoted β-catenin degradation, could rescue the inhibition (Figure 4E). Furthermore, we overexpressed human *UCP1*-promoter-driven luciferase and human TCF7L2, the transcription factor that formed a transcriptional complex with β-catenin, in 293T cells, and the transcriptional activity of h*UCP1* promoter was also dramatically inhibited

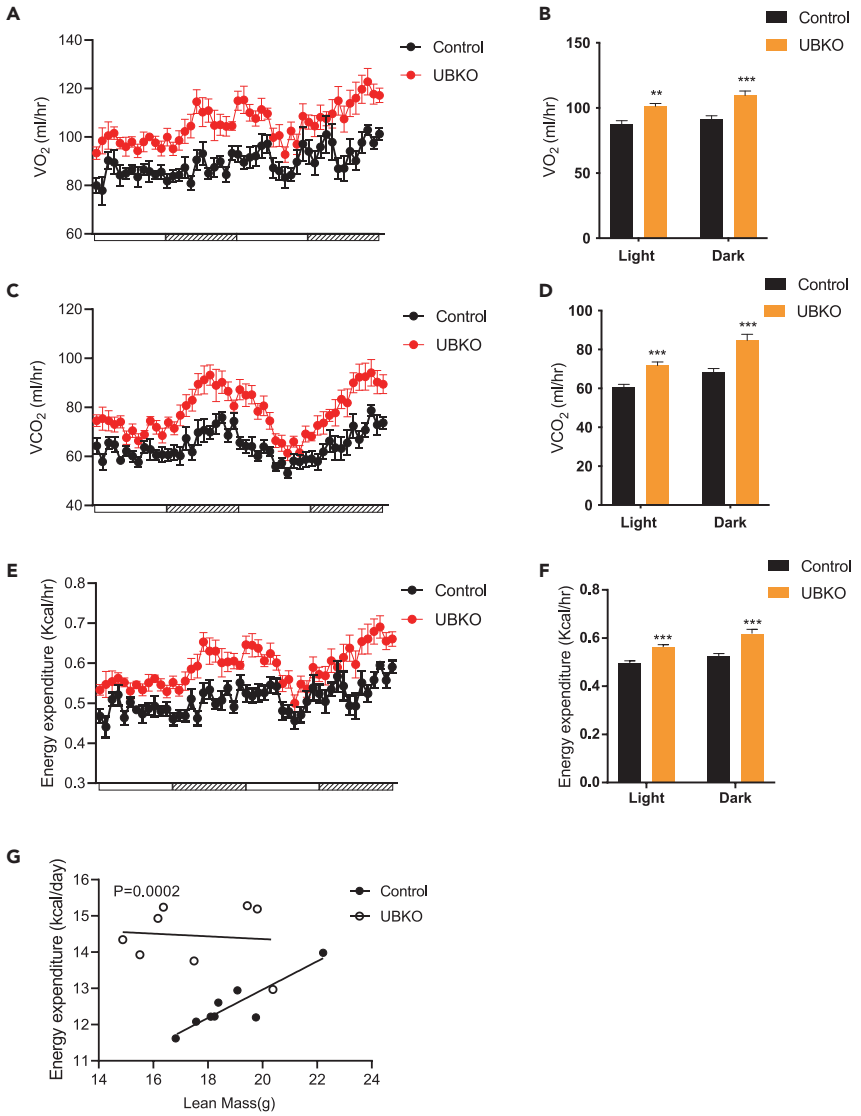

Figure 3. UBKO male mice exhibit increased whole-body energy expenditure at baseline

(A and B) Oxygen consumption was measured in metabolic cages (A) and analyzed during light and dark periods (B) for UBKO and control 8-week-old male mice.

(C and D) Carbon dioxide production was measured (C) and analyzed during the light and dark periods (D).

(E and F) Energy expenditure was measured (E) and calculated during the light and dark period (F).

(G) Energy expenditure was plotted in relation to lean mass using ANCOVA. n = 8 for each group. Data are shown as means ± SEM. *p < 0.05, **p < 0.01, ***p < 0.001. See also Figure S4.

(Figure 4F). These results implied that β-catenin inhibited *Ucp1*-dependent thermogenesis at transcriptional level *in vitro*.

Bulk RNA-seq reveals enhanced mitochondrial functions and decreased inflammation in UBKO mice

To gain a deeper understanding of *Ctnnb1* deficiency in adipose tissue under thermogenic stimuli, we performed RNA-seq analysis on eWAT samples from the control and UBKO group treated with CL-316,243. Principal component analysis was applied to visualize the sample distribution patterns. As shown in Figure 5A, the UBKO group was separated from the control group. Among the 28483 genes that were identified, 290 genes were upregulated (p value <0.05, fold change>1.5) and 1607 were downregulated (p value

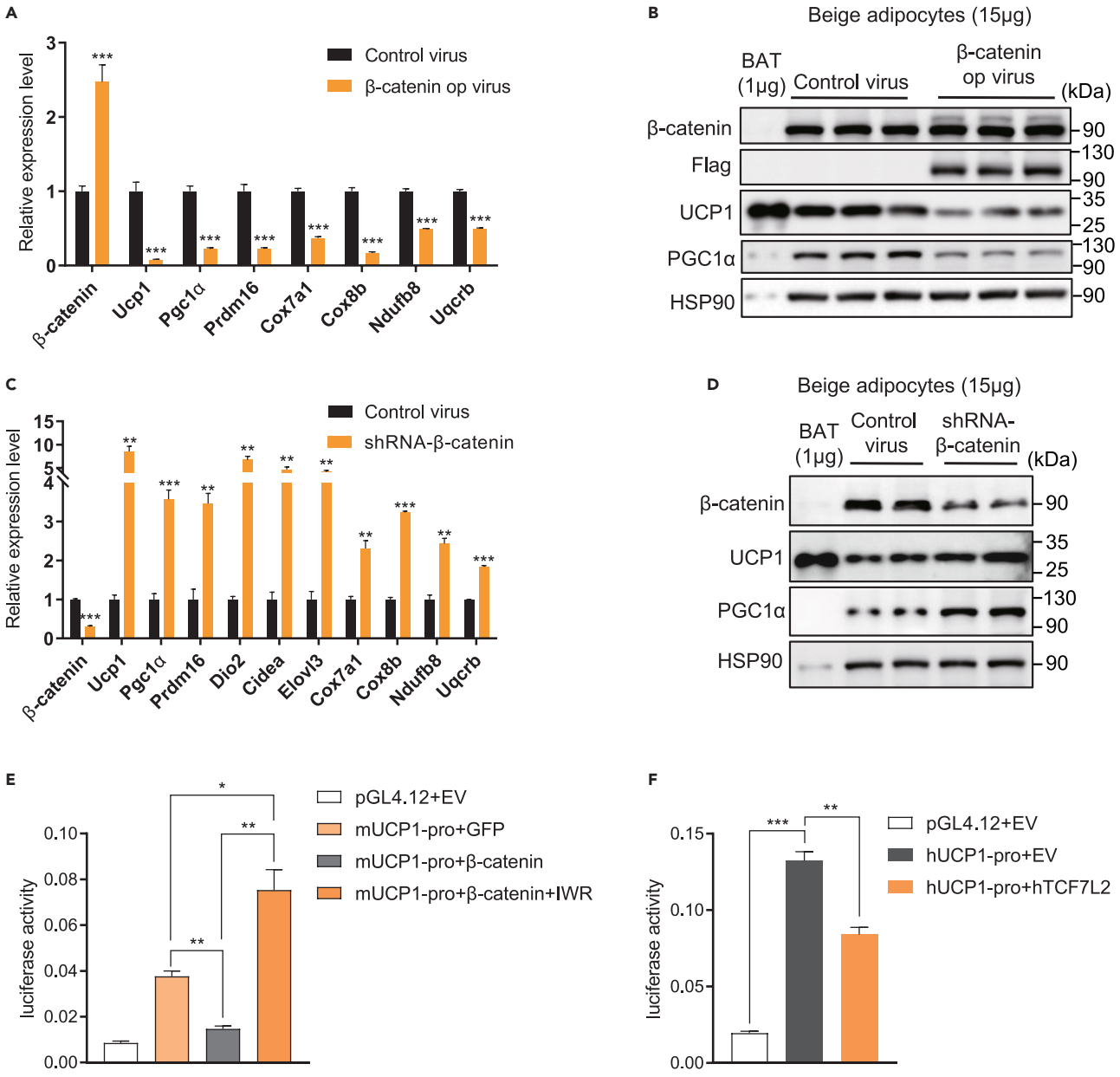

Figure 4. β-catenin inhibits the expression of thermogenic and mitochondria-related genes *in vitro*

(A) mRNA levels of thermogenic and mitochondrial function-associated genes in adenovirus-mediated overexpression of β-catenin in iWAT preadipocytes differentiated for 8 days into beige adipocytes. (n = 6 for each group).

(B) Protein levels of total β-catenin, flag-β-catenin (S33Y/S37F/T41A), UCP1, and PGC1α in induced beige adipocytes from iWAT (15 μg of total protein from cell lysate was loaded onto gel). WT BAT lysate (1 μg) was loaded as a control. (n = 3 for each group).

(C) mRNA levels of thermogenic and mitochondrial function-associated genes in shRNA-mediated knockdown of β-catenin in iWAT preadipocytes differentiated for 8 days into beige adipocytes. (n = 6 for each group).

(D) Protein levels of total β-catenin, UCP1, and PGC1α in induced beige adipocytes from iWAT as in C (15 μg of total protein from cell lysate was loaded onto gel). WT BAT lysate (1 μg) was loaded as a control. (n = 2 for each group).

(E and F) Luciferase reporter assay was performed in 293T cells transfected with the indicated plasmids. pRL-TK (expressing Renilla luciferase) was used as the normalized control. (n = 3 for each group). Data are shown as means ± SEM. *p < 0.05, **p < 0.01, ***p < 0.001. See also Figure S5.

<0.05, fold change<0.67) in the UBKO group, as demonstrated in Figure 5B. The top 25 upregulated and downregulated genes were exhibited in Figure 5C. The results showed that inflammation-related genes such as *Ccl6*, *Ccl9*, and *Cd68* decreased, and genes involved in metabolic pathways such as *Cox8b*,

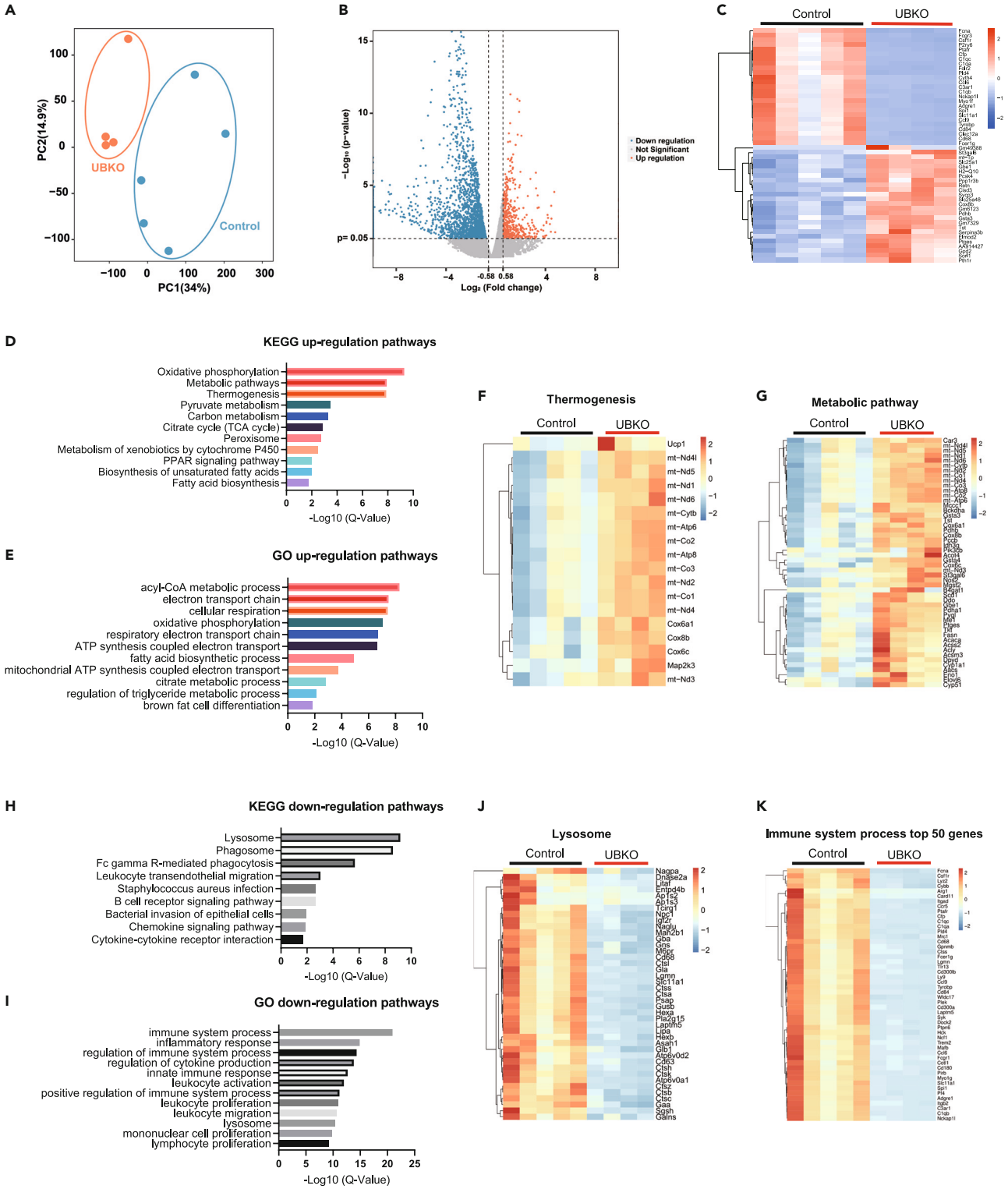

Figure 5. Bulk RNA-seq reveals enhanced mitochondrial functions and decreased inflammation in UBKO mice

(A) Principal component analysis (PCA) of the transcriptome profiles of eWAT of control (blue) and UBKO (orange) mice.

(B) Volcano plot of differentially expressed genes between control and UBKO samples ($p < 0.05$, $|\log_2(FC)|>0.58$).

(C) The heatmap of the top 50 (up and down: top 25 each) genes significantly highly expressed in control or UBKO samples.

(D) Upregulated KEGG pathways between eWAT of control and UBKO group.

Figure 5. *Continued*

(E) Upregulated GO pathways between eWAT of control and UBKO group.

(F) The heatmap of thermogenic genes significantly highly expressed in UBKO samples.

(G) The heatmap of genes involves metabolic pathways that are significantly highly expressed in UBKO samples.

(H) Downregulated KEGG pathways between eWAT of control and UBKO group.

(I) Downregulated GO pathways between eWAT of control and UBKO group.

(J) The heatmap of lysosome-related genes in eWAT of two groups.

(K) The heatmap of the top 50 genes involved in the immune system process in eWAT of two groups. 8-week-old UBKO and control male mice were injected with CL-316,243 for 5 Days n = 4–5 for each group.

mt-Tp, and *Gpd2* increased in the UBKO group. Furthermore, analysis of the gene transcription profiles through KEGG revealed that the upregulated pathways were associated with mitochondrial functions, including oxidative phosphorylation, metabolic pathways, thermogenesis, as well as ATP synthesis coupled electron transport and brown fat cell differentiation (Figure 5D). These results were also verified by Gene Ontology (Figure 5E) and the expression of mitochondria-related genes listed in Figures 5F and 5G. In addition, the downregulated genes were enriched in pathways associated with the lysosome, immune system process, and inflammatory response, as revealed by KEGG and GO analysis (Figures 5H and 5I). Further analysis also confirmed that the downregulated profiles of genes were related to the lysosome and immune system process in the UBKO group (Figures 5J and 5K). Taken together, these results were consistent with our results *in vivo* and *in vitro*, indicating that *Ctnnb1* deficiency in UCP1-positive adipocytes significantly increased mitochondrial functions beyond the thermogenic program. Its deficiency also exhibited potential anti-inflammatory effects in WAT, which may contribute to the improvement of metabolic performance.

Ctnnb1 deficiency in UCP1-positive adipocytes improves metabolic performance in 50-week-old mice

Glucose metabolism deteriorates with aging.[32] To assess the long-term effects of *Ctnnb1* deficiency in brown/beige adipocytes, we investigated changes in body weight and glucose metabolism in 50-week-old UBKO model. The mice were kept on a normal chow diet for 50 weeks. Consistent with previous results, UBKO mice had lower body weight and adipose tissue weight (Figures 6A–6C). Importantly, we performed an intraperitoneal glucose tolerance test and insulin tolerance test, which showed that UBKO mice exhibited better glucose tolerance capacity (Figures 6D and 6E) and insulin sensitivity (Figures 6F and 6G). Although UBKO mice were not exposed to coldness or treated with CL-316,243, some of the thermogenic genes in BAT increased during aging (Figure 6H). *Ucp1*, *Dio2*, *Cidea*, and *Elovl6* were significantly elevated in iWAT of UBKO mice (Figure 6I), while eWAT of UBKO mice showed a mild change in thermogenic genes expression (Figure 6J). Histological analysis of BAT and WAT depots exhibited reduced lipid droplet size (Figures S6A and S6B). Chronic inflammation in WAT induced by aging is a major factor contributing to insulin resistance.[33] We detected proinflammatory macrophage markers and found that the inflammation level decreased in the eWAT of UBKO mice but not in iWAT, which further confirmed the RNA-seq results (Figures 6K and 6L). These results suggested that *Ctnnb1* ablation in brown/beige adipocytes could reduce body weight and improve whole-body glucose metabolism during aging.

CTNNB1 expression inversely correlates with thermogenic genes in human adipocytes

We further analyzed the correlation between the expression of *CTNNB1* and several thermogenic genes in subcutaneous adipose tissue from 770 men of GSE70353.[34] Interestingly, *CTNNB1* had a significant inverse correlation with the expression of *UCP1*, *PRDM16*, and *CIDEA* (Figure 7A, top panel), which was in consistence with our findings in mice. Although it did not show a significant correlation between *CTNNB1* expression and BMI, there was a positive correlation between *CTNNB1* expression with WHR (Figure 7A, bottom panel), suggesting a potential regulatory role of *CTNNB1* on human adipose distribution. MacDougald's group found that the expression of *Ctnnb1* in SVFs would increase when *Ctnnb1* was knocked down in mature adipocytes; therefore, the expression level was relatively stable in whole tissue.[19] According to that, we further analyzed the correlation in mature adipocytes from subcutaneous panniculus adipose[35] and validated the inverse correlation between *CTNNB1* and thermogenic genes expression (Figure 7B, left and middle panels). In addition, *CTNNB1* expression exhibited a significantly positive correlation with BMI in purified adipocytes (Figure 7B, right panel). Collectively, our findings suggested the expression disturbance of *CTNNB1* was associated with enhanced thermogenesis and might contribute to the improvement of metabolic performance.

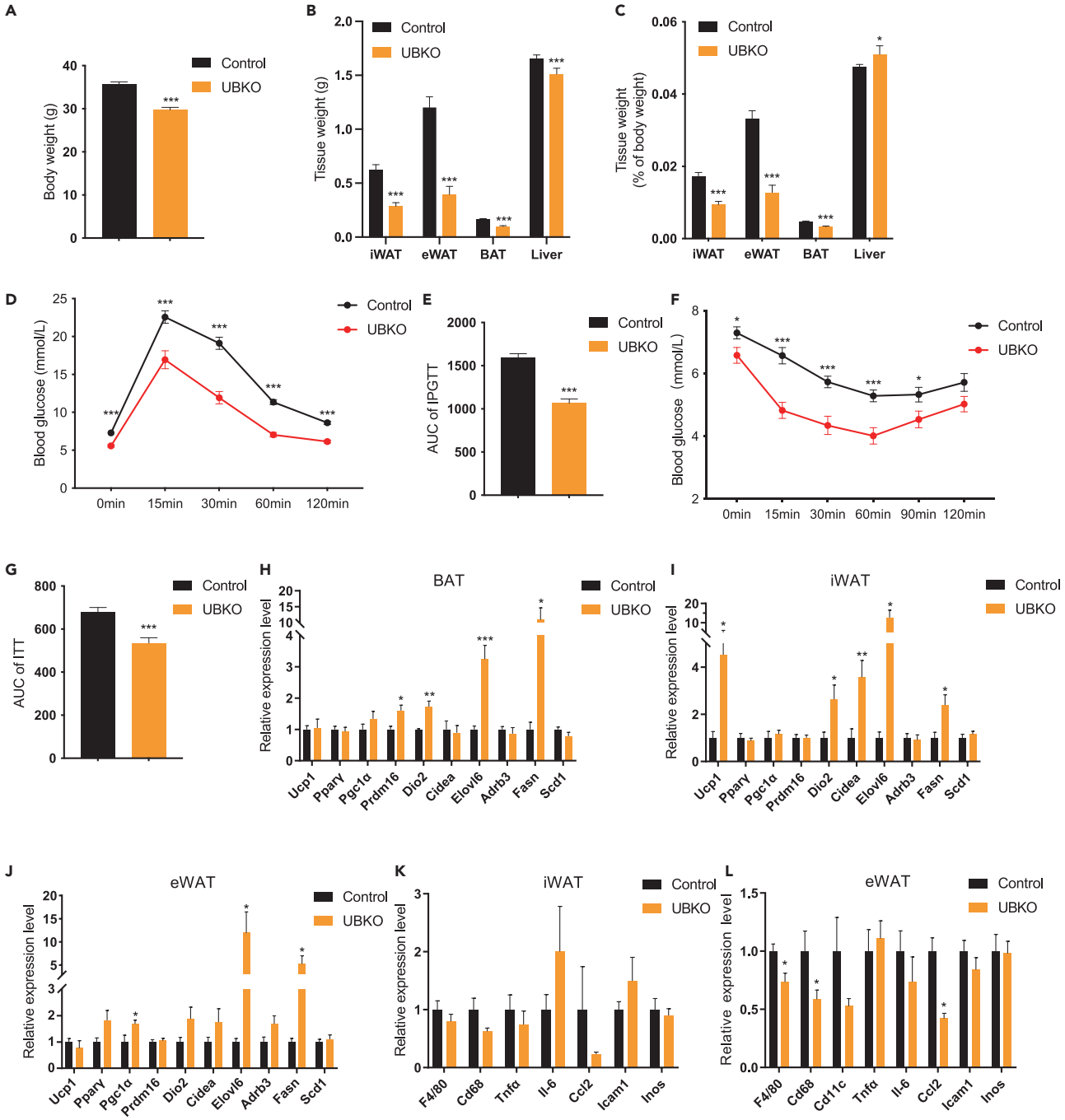

Figure 6. *Ctnnb1* deficiency in UCP1-positive adipocytes improves metabolic performance in 50-week-old mice

(A–C) Body weight (A), tissue weight (B), and percentage of tissue weight (C) of 50-week-old UBKO and control male mice.

(D and E) Glucose tolerance test after 16-h fasting (D) and calculation of area under the curve (AUC) of 10-month-old UBKO and control male mice (E).

(F and G) Insulin tolerance test after 6-h fasting (F) and calculation of AUC (G) of 10-month-old UBKO and control male mice.

(H–J) mRNA levels of thermogenic genes in BAT (H), iWAT (I), and eWAT (J) of 50-week-old UBKO and control male mice.

(K and L) mRNA levels of genes related to inflammation in iWAT (K) and eWAT (L) of 50-week-old UBKO and control male mice. For A–G, n = 25 for the control group, and n = 19 for the UBKO group. For H–L, n = 8 for each group. Data are shown as means ± SEM. *p < 0.05, **p < 0.01, ***p < 0.001. See also Figure S6.

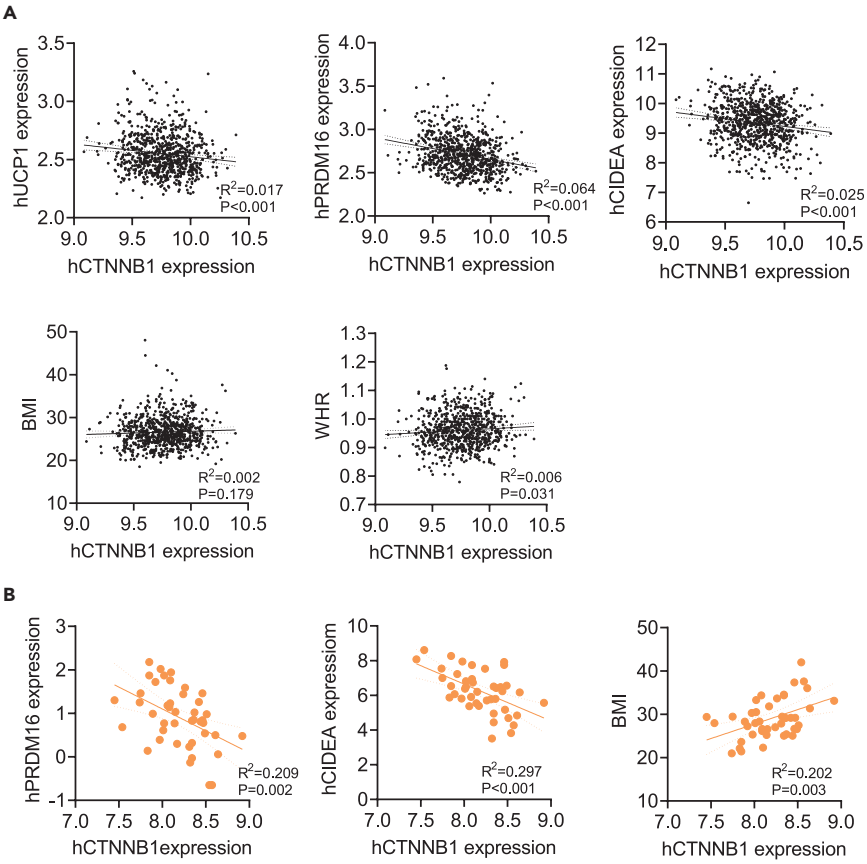

Figure 7. *CTNNB1* expression inversely correlates with thermogenic genes in human adipocytes

(A) Correlation analysis of *UCP1*, *PRDM16*, *CIDEA*, BMI, WHR, and *CTNNB1* expression in subcutaneous adipose from GSE70353 database (n = 770).

(B) Correlation analysis of *PRDM16*, *CIDEA*, BMI, and *CTNNB1* expression in purified adipocytes of subcutaneous adipose from GSE174475 database (n = 43).

DISCUSSION

Beige adipocytes induction has emerged as a promising strategy for combating obesity. In humans, cold exposure or local hyperthermia therapy has been demonstrated to activate beige adipocytes in the supraclavicular region.[36,37] However, the regulatory mechanisms underlying adaptive thermogenesis in beige adipocytes are still not fully clarified. In this study, we demonstrate that ablation of *Ctnnb1* in UCP1-positive adipocytes enhanced energy expenditure, resulting in decreased body weight and improved glucose metabolism by modulating the browning process of WAT.

The canonical WNT pathway has been shown to influence adipogenesis, obesity, and fat distribution.[16,17] A substantial body of literature has focused on the inhibitory effects of canonical WNT signaling during the early stages of adipogenesis.[38–40] In our recent study, we discovered that β-catenin in mature adipocytes exacerbated adipose tissue expansion by regulating the crosstalk among mature adipocytes, macrophages, and preadipocytes during the development of obesity. This suggests that canonical WNT signaling plays distinct roles at different stages of adipocyte development. However, it remains unclear whether β-catenin regulated energy expenditure directly. A previous report demonstrated that *Ucp1*-promoter-driven overexpression of *Wnt10b* inhibited the expression of *Ucp1* and *Pgc1α*, without affecting adipogenic genes such as *Pparγ*, *C/ebpα*, and *Fabp4*, ultimately leading to "whitening" of BAT.[20] Some concerns regarding the relationship between β-catenin and adaptive thermogenesis remain unclear. WNT10b is one of the WNT ligands that are secreted by "producing" cells and functions in a paracrine or autocrine manner.[41] This suggests that WNT10b may have an impact on cell types other than mature adipocytes. In addition, differences in transcription mechanisms between brown adipocytes and beige

adipocytes exist. Furthermore, although β-catenin is typically viewed as a canonical WNT effector, it also participates in other pathways in specific contexts.[42,43] Currently, few studies have investigated the effects of β-catenin on the "browning" of WAT.

Recently, Bagchi et al. found that *Adiponectin*-cre-mediated *Ctnnb1* knockout (ABKO) in BAT resulted in a 50% reduction, but did not affect the expression of the thermogenic protein UCP1.[19] We have also observed this phenomenon in our unpublished work, and furthermore, no differences in WAT browning between ABKO mice and control mice under cold exposure. In 2020, Wolfrum et al. utilized single-nucleus RNA sequencing to identify a subpopulation of adipocytes marked by CYP2E1 that inhibited the thermogenic capacity of neighboring adipocytes.[25] Interestingly, most CYP2E1-positive adipocytes were *Ucp1*-negative. It remains unclear what role β-catenin plays in CYP2E1-positive cells, and whether this is why ABKO mice failed to induce changes in thermogenic genes. It is an intriguing question how β-catenin modulates the function of CYP2E1-positive adipocytes and affects the progress of thermogenesis. In this study, we propose that *Ucp1*-cre is a more suitable mouse model to achieve *Ctnnb1* ablation in UCP1-positive adipocytes to investigate the role of *Ctnnb1* in adaptive thermogenesis.

Bagchi et al. observed that *Adiponectin*-cre-mediated *Ctnnb1* knockout resulted in a compensatory increase of β-catenin expression in neighboring SVF cells.[19] We recently demonstrated that the WNT pathway ligand RSPO1 can activate the downstream β-catenin by binding to the LGR4 receptor in some SVF cells, thereby inhibiting the browning of WAT.[44] These findings imply that the increase in β-catenin expression in SVF cells may offset the enhancement of WAT browning induced by *Ctnnb1* knockout. In this study, the immunofluorescence staining did not reveal any significant compensatory effect. This could be attributed to the relatively small percentage of UCP1-positive cells in WAT, and the minor perturbation of β-catenin expression at the tissue level might not be sufficient to trigger compensatory expression in SVF cells.

Both brown and beige adipocytes share similar morphological features, common markers, and core transcription factors such as *Pparγ*, *Pgc1α*, and *Prdm16*.[45] However, we found that *Ctnnb1* deletion did not affect the expression of thermogenic genes in BAT, whereas the "browning" of WAT was robustly induced under both cold exposure and CL-316,243 injection. It is well known that the two types of thermogenic adipocytes originate from different precursor cells, and the expression of UCP1 in BAT is persistent, whereas the formation of beige cells and the expression of UCP1 require specific conditions (such as cold exposure or β3-AR agonist).[8] After the withdrawal of these stimuli, the UCP1 expression in beige cells gradually weakens until it disappears.[46,47] These fat cells induced by stimulation can transform between white and beige fat cells,[46] and β-catenin may play a role in this process of cell identity switching. The transcriptional events in brown and beige adipocytes exhibit some inconsistencies, as previously reported.[48–50] β-catenin acts as a co-transcription factor, and its regulatory function is dependent on its interaction with specific transcription factors to control gene expression.[15] However, a comprehensive analysis of the differential transcription factor binding partners of β-catenin in beige and brown adipocytes has not been conducted. The dissimilarities in transcription factor regulation may underlie distinct thermogenic cellular effects. Further investigation is necessary to elucidate the differences in transcriptome and proteome between brown and beige adipocytes in the absence of *Ctnnb1*.

Cold exposure and CL-316,243 treatment are frequently utilized models to induce WAT browning, but they function via distinct mechanisms. A prior investigation has revealed that cold-induced beige cells primarily emerge from *de novo* adipogenesis, whereas β3-AR activation by CL-316,243 not only modulates the proliferation and differentiation of adipose precursor cells but also drives the transition of white adipocytes into beige adipocytes.[29] In our study, we discovered that the deletion of *Ctnnb1* in UCP1-positive cells increased the expression of thermogenic genes in both models, although the impact on distinct adipose depots was not entirely identical. Our results indicate that in the cold-induced model, the effect of Ctnnb1 knockout on the expression of genes involved in thermogenesis and mitochondrial function is profound in iWAT, which is consistent with the established notion that iWAT is prone to browning;[45] however, in the CL-316,243-induced model, the gene expression is more affected by *Ctnnb1* deletion in eWAT. We hypothesize that this could be attributed to the response of adipose precursor cells to CL-316,243 stimulation, which is observed in eWAT, but not in iWAT.[51]

In addition to the enhanced browning ability of UBKO mice observed under cold exposure and CL-316,243 treatment, it is interesting to note that the energy expenditure of UBKO mice is still significantly higher than

that of control mice under basal conditions at room temperature without any external stimulation. WAT is known to typically lack expression of UCP1 under normal physiological conditions, especially in adult mice. However, previous studies have shown that the browning of WAT can occur spontaneously during the peri-weaning period and persist for about two weeks.[26] This phenomenon is less well studied but important. Our findings suggest that UCP1-positive cells are present in the white fat of mice after weaning, leading to a partial knockout of *Ctnnb1* in UBKO mice. This early-life phenotypic change of UCP1-positive adipocytes in WAT may have significant implications for energy metabolism in adulthood.[26] The mechanisms by which early-life *Ctnnb1* knockout in UCP1-positive cells affects energy and glycolipid metabolism in adulthood require further investigation. In addition, it has been reported that room temperature (22°C) is also a mild cold stimulus for the mice,[52] and in this case it also promotes the browning of WAT. We therefore speculate that this may be a possible reason for the increased level of energy expenditure in UBKO mice at room temperature.

Aging is a well-established risk factor for metabolic disorders such as obesity, glucose intolerance, and type 2 diabetes. Adipose tissue dysfunction is a hallmark of the aging process, and the potential for beige adipocytes formation declines with age.[53] Maintaining the thermogenic capacity of beige adipocytes is an attractive strategy for ameliorating age-related metabolic dysfunction. In this study, we investigated the effects of *Ctnnb1* knockout on metabolic performance in 50-week-old mice. Our findings suggest that *Ctnnb1* deficiency in UCP1-positive adipocytes can partially reverse age-related adipose tissue dysfunction and improve glucose metabolism. To shed light on the underlying mechanisms, we postulate that, in addition to the impact of *Ctnnb1* knockout in UCP1-positive cells during early life, our 50-week-old mice have been housed at 22°C, which has been shown to represent a mild cold stimulus for mice[52] and could also influence the expression of thermogenic genes in WAT. Further investigations are needed to determine how different temperatures and durations of cold exposure may affect the regulation of *Ctnnb1* in the browning of WAT.

The canonical WNT pathway is closely associated with the development of obesity. Notably, a given molecule may have multiple roles in different stages of adipogenesis. Our findings contribute to a better understanding of how β-catenin regulates adipose energy expenditure and exacerbates obesity development.

Limitations of the study

We used *Ucp1*-cre in this study to induce *Ctnnb1* knockout in UCP1-positive adipocytes. Our findings indicate a significant increase in cold exposure and β3-AR agonist-induced WAT browning, suggesting that *Ctnnb1*/β-catenin is a crucial transcription factor that regulates the browning process. However, several limitations were encountered in this study. We could not provide conclusive experimental evidence explaining the differential effects of *Ctnnb1* knockout on classical brown adipocytes and beige adipocytes. In addition, a transcription factor that interacts with *Ctnnb1* and co-regulates the transcription of *Ucp1* in beige adipocytes has not yet been identified. It is hypothesized that *Ctnnb1* knockout in WAT during the peri-weaning period may influence energy expenditure in adulthood and improve glucose metabolism in old age. However, sufficient experimental evidence is lacking, and future studies are needed to solve the above limitations.

STAR★METHODS

Detailed methods are provided in the online version of this paper and include the following:

- KEY RESOURCES TABLE
- RESOURCE AVAILABILITY
  - Lead contact
  - Materials availability
  - Data and code availability
- EXPERIMENTAL MODEL AND SUBJECT DETAILS
  - Animal models
  - Cold exposure and CL-316,243 injection
  - SVFs isolation and Beige/Brown adipocyte differentiation
- METHOD DETAILS
  - RNA isolation and quantitative PCR analysis
  - Western Blot

- H&E staining and multiplex immunohistochemistry
- Adenovirus and lentivirus generation
- Plasmids and luciferase reporter assay
- RNA-seq

- QUANTIFICATION AND STATISTICAL ANALYSIS

SUPPLEMENTAL INFORMATION

Supplemental information can be found online at https://doi.org/10.1016/j.isci.2023.106552.

ACKNOWLEDGMENTS

This work was supported by grants from the National Natural Science Foundation of China (82200947).

AUTHOR CONTRIBUTIONS

P.L., J.W., and R.L. designed the experiments and supervised the study. P.L., N.C., M.Y., and N.Z. carried out the animal and molecular experiments. N.C. analyzed the GEO data. P.L., J.W., and R.L. analyzed all the experimental data. M.C., R.L., and J.W. provided supports in animal model tests. P.L., N.C., and M.Y. wrote the manuscript. J.W. and R.L. contributed to text revision and discussion.

DECLARATION OF INTERESTS

The authors declare no competing interests.

INCLUSION AND DIVERSITY

We support inclusive, diverse, and equitable conduct of research.

Received: December 6, 2022
Revised: March 9, 2023
Accepted: March 28, 2023
Published: April 1, 2023

REFERENCES

1. Friedrich, M.J. (2017). Global obesity epidemic worsening. JAMA *318*, 603. https://doi.org/10.1001/jama.2017.10693.

2. Jebeile, H., Kelly, A.S., O'Malley, G., and Baur, L.A. (2022). Obesity in children and adolescents: epidemiology, causes, assessment, and management. Lancet Diabetes Endocrinol. *10*, 351–365. https://doi.org/10.1016/s2213-8587(22)00047-x.

3. Cardel, M.I., Atkinson, M.A., Taveras, E.M., Holm, J.C., and Kelly, A.S. (2020). Obesity treatment among adolescents: a review of current evidence and future directions. JAMA Pediatr. *174*, 609–617. https://doi.org/10.1001/jamapediatrics.2020.0085.

4. Leitner, B.P., Huang, S., Brychta, R.J., Duckworth, C.J., Baskin, A.S., McGehee, S., Tal, I., Dieckmann, W., Gupta, G., Kolodny, G.M., et al. (2017). Mapping of human brown adipose tissue in lean and obese young men. Proc. Natl. Acad. Sci. USA *114*, 8649–8654. https://doi.org/10.1073/pnas.1705287114.

5. Kuryłowicz, A., and Puzianowska-Kuźnicka, M. (2020). Induction of adipose tissue browning as a strategy to combat obesity. Int. J. Mol. Sci. *21*, 6241. https://doi.org/10.3390/ijms21176241.

6. Hiradate, R., Khalil, I.A., Matsuda, A., Sasaki, M., Hida, K., and Harashima, H. (2021). A novel dual-targeted rosiglitazone-loaded nanoparticle for the prevention of diet-induced obesity via the browning of white adipose tissue. J. Control. Release *329*, 665–675. https://doi.org/10.1016/j.jconrel.2020.10.002.

7. O'Mara, A.E., Johnson, J.W., Linderman, J.D., Brychta, R.J., McGehee, S., Fletcher, L.A., Fink, Y.A., Kapuria, D., Cassimatis, T.M., Kelsey, N., et al. (2020). Chronic mirabegron treatment increases human brown fat, HDL cholesterol, and insulin sensitivity. J. Clin. Invest. *130*, 2209–2219. https://doi.org/10.1172/JCI131126.

8. Shamsi, F., Wang, C.H., and Tseng, Y.H. (2021). The evolving view of thermogenic adipocytes - ontogeny, niche and function. Nat. Rev. Endocrinol. *17*, 726–744. https://doi.org/10.1038/s41574-021-00562-6.

9. Wu, J., Boström, P., Sparks, L.M., Ye, L., Choi, J.H., Giang, A.H., Khandekar, M., Virtanen, K.A., Nuutila, P., Schaart, G., et al. (2012). Beige adipocytes are a distinct type of thermogenic fat cell in mouse and human. Cell *150*, 366–376. https://doi.org/10.1016/j.cell.2012.05.016.

10. Long, J.Z., Svensson, K.J., Tsai, L., Zeng, X., Roh, H.C., Kong, X., Rao, R.R., Lou, J., Lokurkar, I., Baur, W., et al. (2014). A smooth muscle-like origin for beige adipocytes. Cell Metab. *19*, 810–820. https://doi.org/10.1016/j.cmet.2014.03.025.

11. Cohen, P., and Kajimura, S. (2021). The cellular and functional complexity of thermogenic fat. Nat. Rev. Mol. Cell Biol. *22*, 393–409. https://doi.org/10.1038/s41580-021-00350-0.

12. Ikeda, K., Kang, Q., Yoneshiro, T., Camporez, J.P., Maki, H., Homma, M., Shinoda, K., Chen, Y., Lu, X., Maretich, P., et al. (2017). UCP1-independent signaling involving SERCA2b-mediated calcium cycling regulates beige fat thermogenesis and systemic glucose homeostasis. Nat. Med. *23*, 1454–1465. https://doi.org/10.1038/nm.4429.

13. Shapira, S.N., and Seale, P. (2019). Transcriptional control of Brown and beige fat development and function. Obesity *27*, 13–21. https://doi.org/10.1002/oby.22334.

14. de Winter, T.J.J., and Nusse, R. (2021). Running against the Wnt: how wnt/β-catenin suppresses adipogenesis. Front. Cell Dev. Biol. *9*, 627429. https://doi.org/10.3389/fcell.2021.627429.

15. Perugorria, M.J., Olaizola, P., Labiano, I., Esparza-Baquer, A., Marzioni, M., Marin, J.J.G., Bujanda, L., and Banales, J.M. (2019). Wnt-β-catenin signalling in liver development, health and disease. Nat. Rev.

Gastroenterol. Hepatol. *16*, 121–136. https://doi.org/10.1038/s41575-018-0075-9.

16. Zhang, N., Yuan, M., and Wang, J. (2023). LGR4: a new receptor member in endocrine and metabolic diseases. Endocr. Rev. bnad003. https://doi.org/10.1210/endrev/bnad003.

17. Chen, N., and Wang, J. (2018). Wnt/β-Catenin signaling and obesity. Front. Physiol. *9*, 792. https://doi.org/10.3389/fphys.2018.00792.

18. Chen, M., Lu, P., Ma, Q., Cao, Y., Chen, N., Li, W., Zhao, S., Chen, B., Shi, J., Sun, Y., et al. (2020). CTNNB1/beta-catenin dysfunction contributes to adiposity by regulating the cross-talk of mature adipocytes and preadipocytes. Sci. Adv. *6*, eaax9605. https://doi.org/10.1126/sciadv.aax9605.

19. Bagchi, D.P., Nishii, A., Li, Z., DelProposto, J.B., Corsa, C.A., Mori, H., Hardij, J., Learman, B.S., Lumeng, C.N., and MacDougald, O.A. (2020). Wnt/beta-catenin signaling regulates adipose tissue lipogenesis and adipocyte-specific loss is rigorously defended by neighboring stromal-vascular cells. Mol. Metab. *42*, 101078. https://doi.org/10.1016/j.molmet.2020.101078.

20. Kang, S., Bajnok, L., Longo, K.A., Petersen, R.K., Hansen, J.B., Kristiansen, K., and MacDougald, O.A. (2005). Effects of Wnt signaling on brown adipocyte differentiation and metabolism mediated by PGC-1alpha. Mol. Cell Biol. *25*, 1272–1282. https://doi.org/10.1128/MCB.25.4.1272-1282.2005.

21. Wang, J., Liu, R., Wang, F., Hong, J., Li, X., Chen, M., Ke, Y., Zhang, X., Ma, Q., Wang, R., et al. (2013). Ablation of LGR4 promotes energy expenditure by driving white-to-brown fat switch. Nat. Cell Biol. *15*, 1455–1463. https://doi.org/10.1038/ncb2867.

22. Loh, N.Y., Neville, M.J., Marinou, K., Hardcastle, S.A., Fielding, B.A., Duncan, E.L., McCarthy, M.I., Tobias, J.H., Gregson, C.L., Karpe, F., and Christodoulides, C. (2015). LRP5 regulates human body fat distribution by modulating adipose progenitor biology in a dose- and depot-specific fashion. Cell Metab. *21*, 262–273. https://doi.org/10.1016/j.cmet.2015.01.009.

23. Loh, N.Y., Minchin, J.E.N., Pinnick, K.E., Verma, M., Todorčević, M., Denton, N., Moustafa, J.E.S., Kemp, J.P., Gregson, C.L., Evans, D.M., et al. (2020). RSPO3 impacts body fat distribution and regulates adipose cell biology in vitro. Nat. Commun. *11*, 2797. https://doi.org/10.1038/s41467-020-16592-z.

24. Heid, I.M., Jackson, A.U., Randall, J.C., Winkler, T.W., Qi, L., Steinthorsdottir, V., Thorleifsson, G., Zillikens, M.C., Speliotes, E.K., Mägi, R., et al. (2010). Meta-analysis identifies 13 new loci associated with waist-hip ratio and reveals sexual dimorphism in the genetic basis of fat distribution. Nat. Genet. *42*, 949–960. https://doi.org/10.1038/ng.685.

25. Sun, W., Dong, H., Balaz, M., Slyper, M., Drokhlyansky, E., Colleluori, G., Giordano, A., Kovanicova, Z., Stefanicka, P., Balazova, L., et al. (2020). snRNA-seq reveals a subpopulation of adipocytes that regulates thermogenesis. Nature *587*, 98–102. https://doi.org/10.1038/s41586-020-2856-x.

26. Wu, Y., Kinnebrew, M.A., Kutyavin, V.I., and Chawla, A. (2020). Distinct signaling and transcriptional pathways regulate peri-weaning development and cold-induced recruitment of beige adipocytes. Proc. Natl. Acad. Sci. USA *117*, 6883–6889. https://doi.org/10.1073/pnas.1920419117.

27. Wang, Q.A., Tao, C., Gupta, R.K., and Scherer, P.E. (2013). Tracking adipogenesis during white adipose tissue development, expansion and regeneration. Nat. Med. *19*, 1338–1344. https://doi.org/10.1038/nm.3324.

28. Rosenwald, M., Perdikari, A., Rülicke, T., and Wolfrum, C. (2013). Bi-directional interconversion of brite and white adipocytes. Nat. Cell Biol. *15*, 659–667. https://doi.org/10.1038/ncb2740.

29. Jiang, Y., Berry, D.C., and Graff, J.M. (2017). Distinct cellular and molecular mechanisms for beta3 adrenergic receptor-induced beige adipocyte formation. Elife *6*, e30329. https://doi.org/10.7554/eLife.30329.

30. Hahn, J.Y., Cho, H.J., Bae, J.W., Yuk, H.S., Kim, K.I., Park, K.W., Koo, B.K., Chae, I.H., Shin, C.S., Oh, B.H., et al. (2006). Beta-catenin overexpression reduces myocardial infarct size through differential effects on cardiomyocytes and cardiac fibroblasts. J. Biol. Chem. *281*, 30979–30989. https://doi.org/10.1074/jbc.M603916200.

31. Yang, Y.Y., Zhou, Y.M., Xu, J.Z., Sun, L.H., Tao, B., Wang, W.Q., Wang, J.Q., Zhao, H.Y., and Liu, J.M. (2021). Lgr4 promotes aerobic glycolysis and differentiation in osteoblasts via the canonical Wnt/β-catenin pathway. J. Bone Miner. Res. *36*, 1605–1620. https://doi.org/10.1002/jbmr.4321.

32. Kalyani, R.R., and Egan, J.M. (2013). Diabetes and altered glucose metabolism with aging. Endocrinol. Metab. Clin. North Am. *42*, 333–347. https://doi.org/10.1016/j.ecl.2013.02.010.

33. Wu, D., Ren, Z., Pae, M., Guo, W., Cui, X., Merrill, A.H., and Meydani, S.N. (2007). Aging up-regulates expression of inflammatory mediators in mouse adipose tissue. J. Immunol. *179*, 4829–4839. https://doi.org/10.4049/jimmunol.179.7.4829.

34. Civelek, M., Wu, Y., Pan, C., Raulerson, C.K., Ko, A., He, A., Tilford, C., Saleem, N.K., Stančáková, A., Scott, L.J., et al. (2017). Genetic regulation of adipose gene expression and cardio-metabolic traits. Am. J. Hum. Genet. *100*, 428–443. https://doi.org/10.1016/j.ajhg.2017.01.027.

35. Emont, M.P., Jacobs, C., Essene, A.L., Pant, D., Tenen, D., Colleluori, G., Di Vincenzo, A., Jørgensen, A.M., Dashti, H., Stefek, A., et al. (2022). A single-cell atlas of human and mouse white adipose tissue. Nature *603*, 926–933.

36. van Marken Lichtenbelt, W.D., Vanhommerig, J.W., Smulders, N.M., Drossaerts, J.M.A.F.L., Kemerink, G.J., Bouvy, N.D., Schrauwen, P., and Teule, G.J.J. (2009). Cold-activated brown adipose tissue in healthy men. N. Engl. J. Med. *360*, 1500–1508. https://doi.org/10.1056/NEJMoa0808718.

37. Li, Y., Wang, D., Ping, X., Zhang, Y., Zhang, T., Wang, L., Jin, L., Zhao, W., Guo, M., Shen, F., et al. (2022). Local hyperthermia therapy induces browning of white fat and treats obesity. Cell *185*, 949–966.e19. https://doi.org/10.1016/j.cell.2022.02.004.

38. Christodoulides, C., Laudes, M., Cawthorn, W.P., Schinner, S., Soos, M., O'Rahilly, S., Sethi, J.K., and Vidal-Puig, A. (2006). The Wnt antagonist Dickkopf-1 and its receptors are coordinately regulated during early human adipogenesis. J. Cell Sci. *119*, 2613–2620. https://doi.org/10.1242/jcs.02975.

39. Takemaru, K.I., Yamaguchi, S., Lee, Y.S., Zhang, Y., Carthew, R.W., and Moon, R.T. (2003). Chibby, a nuclear beta-catenin-associated antagonist of the Wnt/Wingless pathway. Nature *422*, 905–909. https://doi.org/10.1038/nature01570.

40. Villanueva, C.J., Waki, H., Godio, C., Nielsen, R., Chou, W.L., Vargas, L., Wroblewski, K., Schmedt, C., Chao, L.C., Boyadjian, R., et al. (2011). TLE3 is a dual-function transcriptional coregulator of adipogenesis. Cell Metab. *13*, 413–427. https://doi.org/10.1016/j.cmet.2011.02.014.

41. Perkins, R.S., Singh, R., Abell, A.N., Krum, S.A., and Miranda-Carboni, G.A. (2023). The role of WNT10B in physiology and disease: a 10-year update. Front. Cell Dev. Biol. *11*, 1120365. https://doi.org/10.3389/fcell.2023.1120365.

42. Singh, R., Artaza, J.N., Taylor, W.E., Braga, M., Yuan, X., Gonzalez-Cadavid, N.F., and Bhasin, S. (2006). Testosterone inhibits adipogenic differentiation in 3T3-L1 cells: nuclear translocation of androgen receptor complex with beta-catenin and T-cell factor 4 may bypass canonical Wnt signaling to down-regulate adipogenic transcription factors. Endocrinology *147*, 141–154. https://doi.org/10.1210/en.2004-1649.

43. Cawthorn, W.P., Heyd, F., Hegyi, K., and Sethi, J.K. (2007). Tumour necrosis factor-alpha inhibits adipogenesis via a beta-catenin/TCF4(TCF7L2)-dependent pathway. Cell Death Differ. *14*, 1361–1373. https://doi.org/10.1038/sj.cdd.4402127.

44. Sun, Y., Zhang, J., Hong, J., Zhang, Z., Lu, P., Gao, A., Ni, M., Zhang, Z., Yang, H., Shen, J., et al. (2023). Human RSPO1 mutation represses beige adipocyte thermogenesis and contributes to diet-induced adiposity. Adv. Sci. e2207152. https://doi.org/10.1002/advs.202207152.

45. Wang, W., and Seale, P. (2016). Control of brown and beige fat development. Nat. Rev. Mol. Cell Biol. *17*, 691–702. https://doi.org/10.1038/nrm.2016.96.

46. Roh, H.C., Tsai, L.T.Y., Shao, M., Tenen, D., Shen, Y., Kumari, M., Lyubetskaya, A., Jacobs, C., Dawes, B., Gupta, R.K., and Rosen, E.D. (2018). Warming induces significant reprogramming of beige, but not Brown, adipocyte cellular identity. Cell Metab. *27*, 1121–1137.e5. https://doi.org/10.1016/j.cmet.2018.03.005.

47. Altshuler-Keylin, S., Shinoda, K., Hasegawa, Y., Ikeda, K., Hong, H., Kang, Q., Yang, Y., Perera, R.M., Debnath, J., and Kajimura, S. (2016). Beige adipocyte maintenance is regulated by autophagy-induced mitochondrial clearance. Cell Metab. *24*, 402–419. https://doi.org/10.1016/j.cmet.2016.08.002.

48. Bi, P., Shan, T., Liu, W., Yue, F., Yang, X., Liang, X.R., Wang, J., Li, J., Carlesso, N., Liu, X., and Kuang, S. (2014). Inhibition of Notch signaling promotes browning of white adipose tissue and ameliorates obesity. Nat. Med. *20*, 911–918. https://doi.org/10.1038/nm.3615.

49. Vaicik, M.K., Blagajcevic, A., Ye, H., Morse, M.C., Yang, F., Goddi, A., Brey, E.M., and Cohen, R.N. (2018). The absence of laminin α4 in male mice results in enhanced energy expenditure and increased beige subcutaneous adipose tissue. Endocrinology *159*, 356–367. https://doi.org/10.1210/en.2017-00186.

50. Lucchini, F.C., Wueest, S., Challa, T.D., Item, F., Modica, S., Borsigova, M., Haim, Y., Wolfrum, C., Rudich, A., and Konrad, D. (2020). ASK1 inhibits browning of white adipose tissue in obesity. Nat. Commun. *11*, 1642. https://doi.org/10.1038/s41467-020-15483-7.

51. Lee, Y.H., Petkova, A.P., and Granneman, J.G. (2013). Identification of an adipogenic niche for adipose tissue remodeling and restoration. Cell Metab. *18*, 355–367. https://doi.org/10.1016/j.cmet.2013.08.003.

52. Ganeshan, K., and Chawla, A. (2017). Warming the mouse to model human diseases. Nat. Rev. Endocrinol. *13*, 458–465. https://doi.org/10.1038/nrendo.2017.48.

53. Zoico, E., Rubele, S., De Caro, A., Nori, N., Mazzali, G., Fantin, F., Rossi, A., and Zamboni, M. (2019). Brown and beige adipose tissue and aging. Front. Endocrinol. *10*, 368. https://doi.org/10.3389/fendo.2019.00368.

54. Wang, Q., Ishikawa, T., Michiue, T., Zhu, B.L., Guan, D.W., and Maeda, H. (2012). Stability of endogenous reference genes in postmortem human brains for normalization of quantitative real-time PCR data: comprehensive evaluation using geNorm, NormFinder, and BestKeeper. Int. J. Legal Med. *126*, 943–952. https://doi.org/10.1007/s00414-012-0774-7.

55. Fischer, J., Koch, L., Emmerling, C., Vierkotten, J., Peters, T., Brüning, J.C., and Rüther, U. (2009). Inactivation of the Fto gene protects from obesity. Nature *458*, 894–898. https://doi.org/10.1038/nature07848.

56. Hermsen, M., Volk, V., Bräsen, J.H., Geijs, D.J., Gwinner, W., Kers, J., Linmans, J., Schaadt, N.S., Schmitz, J., Steenbergen, E.J., et al. (2021). Quantitative assessment of inflammatory infiltrates in kidney transplant biopsies using multiplex tyramide signal amplification and deep learning. Lab. Invest. *101*, 970–982. https://doi.org/10.1038/s41374-021-00601-w.

57. Zou, Y., Lu, P., Shi, J., Liu, W., Yang, M., Zhao, S., Chen, N., Chen, M., Sun, Y., Gao, A., et al. (2017). IRX3 promotes the browning of white adipocytes and its rare variants are associated with human obesity risk. EBioMedicine *24*, 64–75. https://doi.org/10.1016/j.ebiom.2017.09.010.

58. Robinson, M.D., McCarthy, D.J., and Smyth, G.K. (2010). edgeR: a Bioconductor package for differential expression analysis of digital gene expression data. Bioinformatics *26*, 139–140. https://doi.org/10.1093/bioinformatics/btp616.

59. Wu, T., Hu, E., Xu, S., Chen, M., Guo, P., Dai, Z., Feng, T., Zhou, L., Tang, W., Zhan, L., et al. (2021). clusterProfiler 4.0: a universal enrichment tool for interpreting omics data. Innovation *2*, 100141. https://doi.org/10.1016/j.xinn.2021.100141.

STAR★METHODS

KEY RESOURCES TABLE

REAGENT or RESOURCE	SOURCE	IDENTIFIER
Antibodies		
Rabbit monoclonal anti-HSP90	Cell Signaling Technology	Cat#4877; RRID: AB_2233307
Mouse monoclonal anti-Flag	Sigma	Cat#F1804; RRID: AB_262044
Rabbit polyclonal anti-β-catenin	Cell Signaling Technology	Cat#9562; RRID: AB_331149
Rabbit anti-UCP-1	Abcam	Cat# ab10983; RRID: AB_2241462
Mouse monoclonal anti-PGC-1α	Santa Cruz Biotechnology	Cat#sc-517380; RRID: AB_2755043
Anti-rabbit IgG, HRP-linked Antibody	Cell Signaling Technology	Cat#7074; RRID: AB_2099233
Anti-mouse IgG, HRP-linked Antibody	Cell Signaling Technology	Cat#7076; RRID: AB_330924
Chemicals, peptides, and recombinant proteins		
CI-316, 243	Sigma	Cat#C5976
IWR-1-endo	Sigma	Cat#681669
Dulbecco's modified Eagle's medium (DMEM), high glucose, pyruvate	Gibco	Cat#11995040
DMEM/F12	Gibco	Cat#11320082
Fetal bovine serum (FBS)	Gibco	Cat#16140071
Recombinant Mouse FGF basic/FGF2/bFGF Protein	R&D Systems	Cat#3139-FB-025
Penicillin-streptomycin solution	Gibco	Cat#15140122
L-glutamine	Gibco	Cat#25030164
1X Phosphate-Buffered Saline (PBS)	Meilunbio	Cat#MA0015
Trypsin-EDTA (0.05%)	Gibco	Cat#25300062
Isobutyl methylxanthine (IBMX)	Sigma	Cat#I7018
Dexamethasone	Sigma	Cat#D4902
Rosiglitazone	Sigma	Cat#R2408
Insulin	Novo nordisk	N/A
3,3',5-Triiodo-L-thyronine	Sigma	Cat#T2877
Collagenase from *Clostridium histolyticum* type II	Sigma	Cat#C6885
HEPES(1M)	Gibco	Cat#15630080
Polybrene Infection	Sigma	Cat#TR1003
Lipofectamine™ 2000 Transfection Reagent	Invitrogen	Cat#11668019
Protease and Phosphatase Inhibitor Cocktail	Thermo Fisher Scientific	Cat# 78441
RIPA lysis buffer	Biocolor	Cat#R20095
Protein Sample Loading Buffer	Yamei	Cat#LT103
Bovine serum albumin (BSA)	GBCBIO	Cat#0332
TBS/Tween Buffer (TBST)	Yamei	Cat#PS103
Western Lightning Plus, Chemiluminescent Substrate	PerkinElmer	Cat#NEL104001EA
TRIzol Reagent	Thermo Fisher scientific	Cat#15596018
PrimeScript RT Master Mix (Perfect Real Time)	Takara	Cat#RR036
ChamQ Universal SYBR qPCR Master Mix	Vazyme	Cat#Q711

(*Continued on next page*)

Continued

REAGENT or RESOURCE	SOURCE	IDENTIFIER
Critical commercial assays		
BCA Protein Assay Kit	Thermo Fisher scientific	Cat#23227
Super Total RNA Extraction Kit	Promega	Cat#LS1040
Dual-luciferase reporter assay system	Promega	Cat#E1910
mRNA-seq Lib Prep Kit for Illumina	ABclonal	Cat#RK20302
Deposited data		
Raw and analyzed data	This paper	GEO: GSE227415
Experimental models: Cell lines		
HEK 293T	American Type Culture Collection	Cat#CLR-11268
Mouse: Stromal-vascular fraction cells	This paper	N/A
Experimental models: Organisms/strains		
Mice: C57BL/6	Cyagen Biosciences (Suzhou)	N/A
Mice: Ucp1-Cre	Jackson Laboratory	JAX stock: 024670
Mice: Ctnnb1$^{flox/flox}$	Jackson Laboratory	JAX stock: 004152
Mice: Ucp1-cre; Ctnnb1$^{flox/flox}$	This paper	N/A
Oligonucleotides		
Primers for qPCR, see Table S1	This paper	N/A
Recombinant DNA		
Plasmid: pcDNA3.1	Invitrogen	Cat#V79520
Plasmid: pGL4.12	Promega	Cat#E6671
Plasmid: pGL4.12-UCP1 promoter	This paper	N/A
Plasmid: pRL-TK	Promega	Cat#E2241
Software and algorithms		
GraphPad Prism (v9.0.0)	GraphPad	http://www.graphpad.com/scientific-software/prism/
SPSS Statistics (v23.0)	IBM	https://www.ibm.com/products/spss-statistics
R (v4.0.0)	N/A	https://www.r-project.org/
edgeR (v3.14)	Bioconductor	https://bioconductor.org/packages/release/bioc/html/edgeR.html
ClusterProfiler (v4.0.0)	Bioconductor	https://bioconductor.org/packages/release/bioc/html/clusterProfiler.html
Other		
Rectal Probe	Physitemp	N/A
PVDF membranes	Bio-rad	Cat#1620177
40 μm strainer	FALCON	Cat#352340
Metabolic Chamber-Comprehensive Lab Animal Monitoring System (CLAMS)	Columbus Instruments	N/A
QuantStudio Dx Real-Time PCR Instrument	Thermo Fisher Scientific	N/A
NanoDrop ND2000 spectrophotometer	Thermo Fisher Scientific	N/A
Illumina NovaSeq 6000 System	Illumina	N/A
TissueFAXS Plus	TissueGnostics GmbH, Austria	N/A

RESOURCE AVAILABILITY

Lead contact

Further information and requests for resources and reagents should be directed to and will be fulfilled by the lead contact, Peng Lu (sibslp@126.com).

Materials availability

The study did not generate new unique reagents. All mouse lines and plasmids generated in this study are available from the lead contact with a completed Materials Transfer Agreement.

Data and code availability

- The transcriptomic data generated in this study have been deposited to NCBI GEO database. The accession number is GSE227415.
- This paper does not report original code.
- Any additional information required to reanalyze the data reported in this paper is available from the lead contact upon request.

EXPERIMENTAL MODEL AND SUBJECT DETAILS

Animal models

UBKO mice were generated using the Cre/*LoxP* system. Briefly, *Ctnnb1*$^{flox/flox}$ mice were mated with *Ucp1*-cre mice, *Ctnnb1*$^{flox/flox}$ mice were used as control mice. Postnatal day 25 (P25) mice were used for investigating the spontaneous browning of WAT at peri-weaning. The long-term effects of *Ctnnb1* deficiency in brown/beige adipocytes were investigated in 50-week-old and 10-month-old mice. 8-week-old mice were used in other studies. Ages are specified in the text or figure legends. Mice were kept under 12-h dark-light cycles with unlimited access to food and water. Ages and sexes of mice are specified in the text or figure legends. EchoMRI was used to analyze the body composition of awake animals. To evaluate systemic energy metabolism, male mice were placed in metabolic cages (Columbus Instruments) to measure O_2 consumption, CO_2 production, RER, physical activity, and energy expenditure. Male mice were used in the experiments. All procedures were proved by the Animal Care Committee of Shanghai Jiao Tong University School of Medicine.

Cold exposure and CL-316,243 injection

Mice were kept individually at 4°C for 7 days to achieve chronic cold exposure. Food and water were free to access. A rectal probe (Physitemp Instruments Inc., USA) was used to detect core body temperature. CL-316,243 (Sigma-Aldrich, USA) was injected intraperitoneally daily at a dose of 1 mg/kg for consecutive 5 days. Mice were maintained at room temperature with free access to food and water.

SVFs isolation and Beige/Brown adipocyte differentiation

Stromal vascular fractions (SVFs) were isolated as previously described.[18] Briefly, iWATs were minced and digested with type II collagenase (2 mg/mL, Sigma-Aldrich). The sample was incubated in a shaker incubator at 37°C for 30 min. Cell suspensions were centrifuged at 800×g for 10 min at 4°C. The pellet was resuspended and filtered through a 40 μm cell strainer (FALCON). The SVFs were then seeded in culture dishes. To conduct beige/brown adipocyte differentiation, primary preadipocytes were cultured with a cocktail medium containing 5 μg/mL insulin, 1 μM dexamethasone, 1 μM rosiglitazone, 1 μM triiodothyronine (T3), and 0.5 mM IBMX (all Sigma–Aldrich, USA) for two days, and subsequently in medium with insulin, rosiglitazone, and T3 for another six days.

METHOD DETAILS

RNA isolation and quantitative PCR analysis

Total RNA was extracted from frozen adipose tissue or cultured cells using Ea-step Super Total RNA Extraction Kit (Promega Biotech Co., China). NanoDrop ND2000 spectrophotometer (Thermo Scientific) was used to detect the RNA concentration. Total RNA was transcribed to cDNA using the PrimerScript Reverse Transcript Master Mix (TaKaRa, Japan). Real-time PCR analysis was performed using a QuantStudio Dx Real-Time PCR Instrument (Applied Biosystems). The stability of three candidate reference genes (*Actb*, *36B4*, and *Gapdh*) in adipose/adipocytes was evaluated using NormFinder,[54] and *36B4* was selected as the reference gene for this study. Data were normalized to *36B4* and analyzed using the $\Delta\Delta C_t$ method.

Western Blot

Proteins from 3T3/L1 cells and induced beige adipocytes were extracted with cold RIPA lysis buffer, followed by concentration quantification with the BCA protein Assay Kit (Thermo Fisher Scientific). Western

blotting was performed as previously described.[55] The following antibodies were used: anti-FLAG (Sigma Aldrich, F1804), anti-β-catenin (Cell Signaling Technology, 9562), anti-PGC1α (Santa Cruz, sc-517380), anti-UCP1 (Abcam, ab10983), anti-HSP90 (Cell Signaling Technology, 2144).

H&E staining and multiplex immunohistochemistry

Adipose tissue was paraffin embedded after being fixed in 4% paraformaldehyde in PBS for 24 h at room temperature. Hematoxylin/eosin (HE) was routinely used to stain 5 μm sections. Paraffin-embedded histological slices were deparaffinized and rehydrated before multiplex immunohistochemistry. After being subjected to heat-mediated antigen retrieval, the slides were blocked and successively incubated with anti-β-catenin (Cell Signaling Technology, 9562; 1:200), anti-UCP1 (Abcam, ab10983; 1:1000) antibody, and HRP-conjugated secondary antibody using Tyramide Signal Amplification (TSA) strategy as previously described.[56] The try-488 and try-cy3 were utilized as tyramine conversion reagents. The whole slides were mounted with DAPI Fluoromount-G (Southern Biotech) and scanned with an automated acquisition system TissueFAXS Plus (TissueGnostics GmbH, Austria).

Adenovirus and lentivirus generation

Adenoviruses expressing the triple mutant β-catenin containing three mutations in phosphorylation sites (S33Y/S37F/T41A) were generated using pAdeno-MCMV-3Flag-P2A-EGFP vector. For β-catenin overexpression, primary preadipocytes were infected with adenovirus from day 2–4 of differentiation. Lentiviral murine β-catenin shRNA constructs were made using PLKO-PGK-GFP lentivector. We verified all constructs using DNA sequencing; the sequence of murine β-catenin shRNA was GGACTCAATACCATTCCATTG which was verified in a previous report.[18] To knock down *Ctnnb1*, primary preadipocytes were treated with lentivirus from day 0–2 of differentiation.

Plasmids and luciferase reporter assay

Mouse *Ucp1* promoter (−1500 to transcriptional start site) was amplified from mouse genomic DNA and inserted into the pGL4-basic vector (Promega). Human *UCP1* promoter was described previously.[57] Plasmids encoding mouse *Ctnnb1*/β-catenin and human TCF7L2 were constructed using pcDNA3.1(+)-IRES: EGFP vector. All constructs were verified by DNA sequencing. For the luciferase reporter assay, 293T cells were transfected with the indicated plasmids for 36 h, treated with IWR-1-endo (5 μM) for 4 h before harvest, followed by luciferase activity measurement using a dual-luciferase reporter assay system (Promega).

RNA-seq

Total RNA was extracted from adipose tissues using Super Total RNA Extraction Kit. After the concentration and quality of the RNA sample were determined, the mRNA-seq Lib Prep Kit for Illumina (ABclonal, China) was used for synthesizing Paired-end libraries according to Sample Preparation Guide. Briefly, the mRNA is fragmented into small pieces (about 150 bp) by divalent cations at 94°C for 8 min. The cleaved RNA fragments were reverse-transcribed into cDNA. An end repair process including A-tailing and ligation of the adapters was performed. The products were purified and enriched to create a cDNA library. The sequencing was carried out on the Illumina NovaSeq 6000 (Illumina). The construction of the cDNA library and sequencing were performed by Sinotech Genomics Co., Ltd (Shanghai, China). The R package edgeR (v3.14)[58] was used to analyze the expression data to identify differentially expressed genes (DEGs). The Benjamini-Hochberg method was used to correct the P-values at a 5% False Discovery Rate (FDR). DEGs were defined as genes with an adjusted P-value <0.05 and fold change (FC) greater than 1.5 or lower than 0.67 ($|\log_2(FC)|>0.58$) between the two groups. The R package stats' prcomp function was used to perform principal component analysis (PCA). ClusterProfiler package (v4.0.0)[59] was used to perform GO and KEGG enrichment analyses (adjusted P-value <0.05) in the R software 4.0.0 version.

QUANTIFICATION AND STATISTICAL ANALYSIS

Data were shown as mean ± SEM and the results were analyzed by two-tailed t-tests. O_2 consumption, CO_2 production, and energy expenditure were corrected for lean mass. General linear regression and ANCOVA analysis were also performed to examine the correlation between energy expenditure and lean mass. A p value less than 0.05 was considered to be significantly different.